

Phase Transitions of the Classical Hard-Ellipse System

Jacques Vieillard-Baron

Citation: *The Journal of Chemical Physics* **56**, 4729 (1972); doi: 10.1063/1.1676946

View online: <http://dx.doi.org/10.1063/1.1676946>

View Table of Contents: <http://scitation.aip.org/content/aip/journal/jcp/56/10?ver=pdfcov>

Published by the **AIP Publishing**

Articles you may be interested in

[Phase diagram of two-dimensional hard ellipses](#)

J. Chem. Phys. **140**, 204502 (2014); 10.1063/1.4878411

[A Monte Carlo algorithm for studying phase transition in systems of hard rigid rods](#)

AIP Conf. Proc. **1447**, 113 (2012); 10.1063/1.4709907

[Phase transition induced by a shock wave in hard-sphere and hard-disk systems](#)

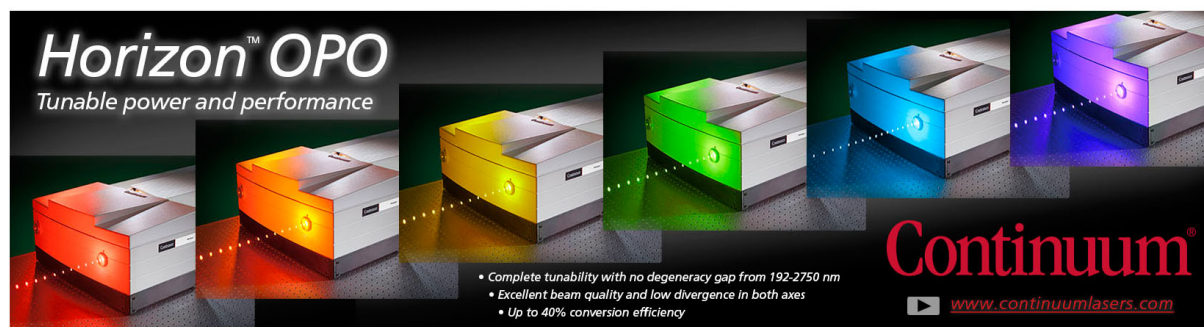
J. Chem. Phys. **129**, 054506 (2008); 10.1063/1.2936990

[A solution to the transition phase in classical novae](#)

AIP Conf. Proc. **637**, 279 (2002); 10.1063/1.1518214

[Phase Transition for a Hard Sphere System](#)

J. Chem. Phys. **27**, 1208 (1957); 10.1063/1.1743957



Horizon™ OPO
Tunable power and performance

- Complete tunability with no degeneracy gap from 192-2750 nm
- Excellent beam quality and low divergence in both axes
- Up to 40% conversion efficiency

Continuum®
www.continuumlasers.com

Phase Transitions of the Classical Hard-Ellipse System

JACQUES VIEILLARD-BARON*

Laboratoire de Physique Théorique et Hautes Energies, Faculté des Sciences, † Orsay, France

(Received 6 July 1970)

By Monte Carlo calculations in the canonical ensemble, we have studied some properties of a two-dimensional system of 170 long hard ellipses (whose axis ratio equals 6). This system can be considered as a two-dimensional model for a nematic liquid crystal. We have shown that this system exhibits two first-order phase transitions: a solid-nematic type phase transition at high density and a disorientation phase transition at a density 1.5 times smaller. This result suggests that excluded volume effects might play an essential role in the disorientation phase transition of nematic liquid crystals.

I. INTRODUCTION

The study of thermodynamical properties of simple classical liquids, such as argon, by the methods of statistical mechanics meets with considerable difficulty. Models which are completely soluble analytically, such as the cell-model, give a very inadequate description of the equation of state of liquids.

Some progress in the understanding of the thermodynamical properties of simple liquids has been achieved recently by use of more realistic models. The solution of these models is obtained by numerical methods (Monte Carlo or molecular dynamics methods) and necessitates the use of fast computers. The model of atoms interacting through a two-body 12-6 Lennard-Jones potential, studied by Wood and Parker,¹ Rahman,² and Verlet,³ among others describes adequately both the equation of state and the phase transitions of argon. As to the hard-sphere system, studied by Alder and Wainwright,⁴ it can be used as a reference system in a perturbation study of the equation of state of liquid argon. Moreover the solidification of the hard-sphere fluid, discovered by these authors, is closely related to the solidification of argon. When the interaction is not spherically symmetric the study of condensed phases is still more difficult. There soluble models present the risk of being very unrealistic and numerical methods seem to be promising.

It is known that some long molecules can exist under three states of different symmetry⁵: between the solid and liquid phases lies an intermediate phase, the so-called nematic phase, in which the molecules have their centers of gravity at random but show some long-range orientational order.

A first-order phase transition separates the nematic from the liquid state. It is tempting to associate this transition with geometrical factors, as is suggested by Onsager's theory.⁶ Onsager's approximation consists of considering the system of long molecules as a mixture, each species of which is made up of the molecules with a definite orientation. Onsager calculates the free energy of the system by using the first two terms of the virial expansion for the mixture, and obtains the distribution function for the orientations of the axes of the molecules by minimizing the free energy. He

thus shows the existence, at sufficiently high density, of an anisotropic phase.

Isihara,⁷ applying Onsager's theory, has predicted the density of the disorientation transition for systems of rigid molecules of ellipsoidal and cylindrical shape.

Zwanzig⁸ has studied a system of infinitely long and thin molecules of parallelepipedic shape, with only three allowed orientations. Let us call l the length of the parallelepiped and d the side of the square basis. In the limit as $l \rightarrow +\infty$ and $d \rightarrow 0$ with l^2d remaining constant (in this limit the volume of each molecule tends to zero), Zwanzig has been able to calculate up to the seventh virial coefficient of the expansion of the free energy in powers of density. The system is considered as a mixture of three species, each species consisting of the molecules of a given orientation. By an extension of Onsager's theory, Zwanzig shows that, at every order of the virial expansion, the system exhibits a van der Waals-like loop associated with the disorientation transition of the parallelepipeds.

Zwanzig's model is somewhat artificial since the volume of each parallelepiped is zero whilst its length is infinite. Moreover, the transition density depends strongly upon the order at which the virial series is truncated. In particular, the van der Waals-like loop nearly vanishes when only six virial coefficients are used.

We have therefore considered a model of a nematic liquid crystal⁵ which is, we hope, somewhat more realistic, namely a system of elastically colliding hard ellipses. We have shown by Monte Carlo calculations in the canonical ensemble that, for sufficiently long ellipses, this system exhibits the following two phase transitions: at high density an order-disorder transition relative to the centers of gravity, analogous to the solid-liquid transition of the hard-disk system,⁹ and, at a lower density, an order-disorder transition relative to the orientations of the ellipses. At high density, the major axes of the ellipses have on the average the same orientation; at a lower density, the ellipses can rotate and the orientational order is destroyed. It should be noted that this orientational order, like the translational order, probably vanishes at very long distance, as in other continuous two-

dimensional systems,¹⁰ in the limit as the number of ellipses becomes infinite: in the systems we have considered, of several hundred ellipses, the order which we observe may be considered as some medium-range order like in the case of solid-liquid transition. The absence of the long-range order does not preclude the existence of a first-order transition.

In the case of ellipses of small eccentricity, as the density is decreased from the close-packed value, the system undergoes the disorientation transition before melting. The intermediate phase which we observe is then analogous to the plastic crystal phase^{11,12}: the ellipses are completely disoriented whilst their centers form a lattice. Note however that, in the plastic crystal phase, the rotational degrees of freedom of the molecules take only discrete values.

In the course of our Monte Carlo computation,¹ we have to select allowed new configurations of the system of ellipses. To do this, we must have a simple and rapid way of determining whether two ellipses of known centers and direction of axes overlap or not. The solution of this problem is given in Sec. II, where we introduce a "contact function" of two ellipses, which is zero when and only when the two ellipses come into contact.

The solution of the corresponding problem in the case of ellipsoids is given in Appendix B. In the case of ellipses, the "contact function" satisfies an inequality, given in Sec. II.B, which enables us to compute the pressure. We have not been able to find a corresponding way to compute the pressure in the case of hard ellipsoids. The study of hard ellipsoids would probably show the existence of different phases in the case of prolate and oblate ellipsoids, the hard-sphere case being in between.

Section III is devoted to the behavior of the hard-ellipse system at very high density. In Sec. III.A we show that this system has a continuous infinity of close-packed configurations which cannot be deduced from one another by displacement. In Sec. III.B we use the free-volume theory to study the asymptotic behavior of the pressure of the system when the area A of the box containing the ellipses approaches its minimum value A_0 . In the free-volume approximation the asymptotic behavior of the pressure is independent of the ratio of the ellipse axes, of the specific close-packed configuration considered (and of the number of ellipses).

In Sec. III.C we study directly the asymptotic behavior of the pressure of a system of N hard ellipses enclosed in a box whose shape is compatible with one of the close-packed configurations, with periodic boundary conditions. We show that, for some close-packed configurations, there are some preferred directions: along these directions, the maximum amplitude by which the ellipses can move (the center of one ellipse being fixed) is an infinitely small quantity of order less than or equal to the order of $[(A/A_0)-1]^{1/2}$,

whereas, along all other directions, this amplitude is of the order of $[(A/A_0)-1]$. In the case of hard disks,¹³ all amplitudes are of order $[(A/A_0)-1]$. At very high density, these displacements of unusually large amplitude probably lower the pressure by a quantity which decreases for large values of N as $1/N^{1/2}$, for a given ratio of axes and shape of the box.

Section IV is devoted to the description of some technical details of the Monte Carlo computation.¹ In Sec. IV.A we describe the method used to compute the pressure, with the help of the contact function introduced in Sec. II. In Sec. IV.B we describe the way in which successive configurations of the system are generated. We indicate in Sec. IV.C the major difficulties which remain in the computation of the pressure in the case of a hard-ellipsoid system.

In Sec. V we describe the solid-nematic and nematic-liquid phase transitions which have been observed for a system of 170 hard ellipses whose axis ratio a/b equals 6 (the box containing these ellipses is nearly square). We give in Sec. V.A the results concerning the melting transition: it takes place at an area A_m/A_0 which decreases when a/b increases, for a nearly fixed number of ellipses N and a nearly unchanged shape of the box. For $a/b=6$ and $N=170$, A_m/A_0 is smaller than 1.15, whereas for a system of 870 hard disks⁹ $A_m/A_0=1.266$.

The nematic-liquid transition, which is also of first order, is described in Sec. V.B. For $a/b=6$ and $N=170$, it starts at area $A_n/A_0=1.775\pm 0.025$. The van der Waals-like loop associated with this transition is very difficult to locate since the liquid and nematic branches of the isotherm lie very close to each other, and the desorientation entropy $\Delta S/Nk$ (k is the Boltzmann's constant) is very small. In the case of hard disks,⁹ the melting entropy is 0.36. Here the desorientation entropy is between 3 and 7 times smaller, due to the fact that the desorientation affects only one degree of freedom per ellipse, instead of two in the case of melting.

In the last section (V.C) we briefly describe the states of the systems of ellipses of weak and very strong eccentricities. We have observed in particular, in the case of a system of 168 hard ellipses with $a/b=1.01$, the onset, at area $A/A_0=1.15$, of a phase analogous to the plastic crystal phase^{11,12} in which the ellipses are oriented at random but with their centers forming a lattice.

II. THE CONTACT FUNCTION OF ELLIPSES

A. Contact Condition for Two Identical Ellipses

In order to select the allowed configurations in the Monte Carlo calculation,¹ one needs to know when two identical ellipses E_1 and E_2 overlap. Let a and b be the length of the major and minor half-axes respectively, \mathbf{u}_1 and \mathbf{u}_2 the unitary vectors of the major axes, $\mathbf{r}=[\mathbf{0}, \mathbf{0}]$ the vector joining the centers O_1 and O_2

of the ellipses. To study the overlap condition of the ellipses we introduce a function $\Psi(\mathbf{r}, \mathbf{u}_1, \mathbf{u}_2; a, b)$ which we call the contact function: $\Psi=0$ when the ellipses are tangent and Ψ is nonzero otherwise. This contact function enables us to determine the pressure and to study the behavior of the system at very high density.

Let \mathbf{u}_1' and \mathbf{u}_2' be the unitary vectors respectively orthogonal to \mathbf{u}_1 and \mathbf{u}_2 , θ the angle between \mathbf{u}_1 and \mathbf{u}_2 : $\theta=(\mathbf{u}_1, \mathbf{u}_2)$. We have proved in Ref. 14 the following statement:

Statement 1. The necessary and sufficient condition for two ellipses E_1 and E_2 to be tangent (interiorly or exteriorly) is $\Psi(\mathbf{r}, \mathbf{u}_1, \mathbf{u}_2; a, b)=0$, where Ψ is defined as follows

$$\Psi=4(f_1^2-3f_2)(f_2^2-3f_1)-(9-f_1f_2)^2, \quad (1a)$$

where ($\alpha=1$ or 2)

$$f_\alpha=1+G-[(\mathbf{r}\cdot\mathbf{u}_\alpha)^2/a^2]-[(\mathbf{r}\cdot\mathbf{u}_\alpha')^2/b^2], \quad (1b)$$

with

$$G=2+[(a/b)-(b/a)]^2 \sin^2\theta. \quad (1c)$$

We have also proved in Ref. 14 the following statement:

Statement 2. The necessary and sufficient condition for two ellipses E_1 and E_2 to have no real point in common is that Ψ be positive and one at least of the two functions f_1 and f_2 be negative.

The outline of the proof of these two statements is given in Appendix A. Statement 2 enables us to select, in the Monte Carlo calculation, the allowed configurations of the hard-ellipse system. We now state an inequality verified by the contact function Ψ which will prove useful in the computation of the pressure described in Sec. IV.A.

B. Comparison of the Contact Function of the Ellipses with the Contact Function of Their Great Circles

In the case of two circles of radius a , which centers distant by r , the contact function Ψ is a function of the ratio r/a only. Using relations (1), one sees that Ψ takes the simple form

$$\Psi_d(r/a)=3(r/a)^6[(r^2/a^2)-4]. \quad (2)$$

When the distance r between the centers O_1 and O_2 of ellipses E_1 and E_2 is greater than $2a$, the ellipses do not overlap. Therefore, when the contact function of their great circles $\Psi_d(r/a)$ is positive, the contact function of the ellipses is also positive, according to Statement 2.

An easy but somewhat long reasoning leads¹⁴ to the following inequality, which proves very useful in the calculation of the pressure

$$\Psi(\mathbf{r}, \mathbf{u}_1, \mathbf{u}_2; a, b) \geq \Psi_d(r/a) \quad \text{for } r \geq 2a > 2b, \quad (3)$$

the equality occurring if and only if the major axes of the ellipses are parallel to the center line O_1O_2 .

III. PROPERTIES OF THE SYSTEM AT VERY HIGH DENSITY

A. The Close-Packed Configurations

Consider a system of N hard ellipses with half-axes a and b . These ellipses are enclosed in a parallelogram-shaped box; we use periodic boundary conditions. In a configuration of maximum density all major axes are likely to be parallel. Let Ox be their common direction and Oy be the orthogonal axis. Consider the following affinity of the close-packed configuration

$$x'=x/a \quad (4a)$$

$$y'=y/b. \quad (4b)$$

It yields a system of N hard disks, of radius unity, enclosed in a box in a close-packed configuration and satisfying the periodic boundary conditions.

Conversely, let us start from this hard-disk configuration (Fig. 1) and apply the affinity inverse of (4); we get a close-packed configuration for the hard-ellipse system. By rotating the coordinate axis Ox before applying the affinity to the hard-disk configuration, one can generate a continuous infinity of close-packed configurations (Fig. 2) which cannot be deduced from one another by displacement. All these configurations have the same maximum density ρ_0 defined by

$$\rho_0 ab = 1/2\sqrt{3}. \quad (5)$$

Thus, any close-packed configuration of the hard-ellipse system is characterized by the angle $\phi_0=(Ox, \llbracket 00_1^{(0)} \rrbracket)$ defined modulo Π in Fig. 1. In the Monte Carlo calculation, we shall always enclose the N ellipses in a box of rectangular shape, as close as possible to a square, compatible, at maximum density, with the lattice of Fig. 2 with either $\phi_0=0$ or $\phi_0=\pi/2$ according to the value of a/b . Such a lattice of ellipses, with their major axes parallel to Ox , is thus characterized by one of the following sets of parameters

$$\phi_0=0; \quad \phi=\pi/2, \quad 00_1^{(0)}=2a, \quad 0_2^{(0)}0_3^{(0)}=2\sqrt{3}b, \quad (6a)$$

$$\phi_0=\pi/2; \quad \phi=\pi/2, \quad 00_1^{(0)}=2b, \quad 0_2^{(0)}0_3^{(0)}=2\sqrt{3}a. \quad (6b)$$

In the case where $\phi_0=0$, the lattice has N_y equidistant lines parallel to $00_1^{(0)}$ (or Ox), each line containing N_x ellipses at contact; (N_y is even because of periodic boundary conditions). When $\phi_0=\pi/2$, the lattice has N_x equidistant rows parallel to $00_1^{(0)}$ (or Oy), each row containing N_y ellipses at contact; (in this case the periodic boundary conditions restrict N_x to even values).

In both cases $\phi=\pi/2$ and the box containing the N ellipses ($N=N_xN_y$) compatible with the close-packed lattice is rectangular. At maximum density

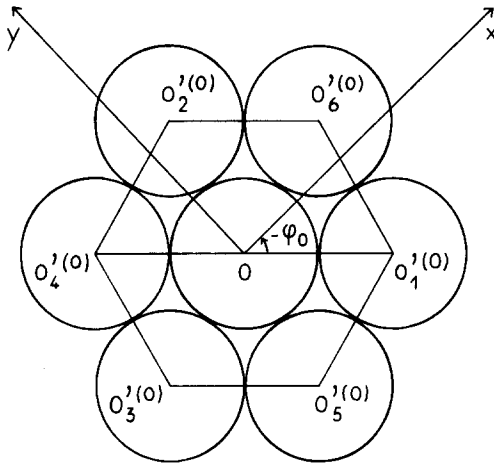


FIG. 1. The hexagonal lattice for hard disks.

the sides of the box have the following length

$$\text{if } \phi_0=0, \quad L_x^{(0)}=2aN_x \quad \text{and} \quad L_y^{(0)}=\sqrt{3}bN_\nu, \quad (7a)$$

$$\text{if } \phi_0=\pi/2, \quad L_x^{(0)}=\sqrt{3}aN_x \quad \text{and} \quad L_y^{(0)}=2bN_\nu. \quad (7b)$$

B. The Free-Volume Theory

We are now interested in determining the asymptotic behavior of the pressure P of the hard-ellipse system as the area A of the box approaches its minimum value $A_0=N/\rho_0$. We shall show that, at very high density, the pressure probably behaves as

$$PA/NkT = \{\nu/[(A/A_0)-1]\} (1+\epsilon_1), \quad (8)$$

with ϵ_1 tending to zero as $A \rightarrow A_0$; ν is a constant depending upon a/b , N and the shape of the box compatible with one of the close-packed lattice drawn on Fig. 2 (T is the absolute temperature which plays no role in the compressibility factor).

One can deduce from (8) the behavior of the partition function Z_N

$$\log Z_N = N\nu \{ \log[(A/A_0)-1] \} [1+\epsilon_2], \quad (9)$$

with ϵ_2 tending to zero when A approaches A_0 .

Let us recall that, in the case of a system of N hard disks enclosed in a box, with periodic boundary conditions,¹³ $\nu=2-(2/N)$. Indeed, due to translational invariance, the total number of degrees of freedom of the hard-disk system is $2N-2$; as $A \rightarrow A_0$, the variations of these degrees of freedom are of the same order as the variation of the size of the box containing the disks, namely $(A/A_0)-1$. The configurational partition function Z_N is therefore an infinitely small quantity of order $[(A/A_0)-1]^{2N-2}$, which by (9) means that $N\nu=2N-2$.

We shall prove that in the free-volume approximation, where the six neighboring ellipses of a given ellipse are fixed, $\nu=3$. In the case of hard disks, the

free-volume theory yields $\nu=2$. The difference comes from the rotation degree of freedom of each ellipse.

As N tends to infinity, always with periodic conditions, the parameter ν appearing in the asymptotic expressions (8) and (9) certainly approaches 3, for any value of the ratio a/b and for any shape of the box compatible with one of the close-packed lattice of Fig. 2. However, as N tends to infinity, the domain of areas A/A_0 for which these asymptotic values are reached within a given accuracy probably depends upon a/b and upon the shape of the box. For instance, for a practically invariant shape of the box, the domain of areas A/A_0 where the asymptotic value (8) is reached tends to zero as $a/b \rightarrow 1$ (for fixed N) or as $a/b \rightarrow +\infty$ (N_ν tending to infinity). Indeed, at fixed density, when $a/b \rightarrow 1$, the ellipses can rotate and the pressure of the hard-ellipse system decreases and approaches the hard-disk value; when $a/b \rightarrow +\infty$ ($N_\nu \rightarrow +\infty$) the lines of the ellipses can slide in a parallel direction to Ox and the pressure P decreases.

In the next section, we shall study the way in which the parameter ν appearing in the asymptotic expressions (8) and (9) depends upon N (for large N), for a given value of a/b and a given shape of the box.

Let us now prove the relation (9) with $\nu=3$ in the case of hard ellipses, by use of the free-volume theory. In a close-packed configuration (Fig. 2), let us consider an ellipse E , initially centered at the origin 0 , and its six nearest neighbors E_j , centered at $O_j^{(0)}$ ($1 \leq j \leq 6$). All the major axes are parallel to Ox . At a lower density A_0/A , the j th lattice site is at point O_j with

$$\mathbf{R}_j = \mathbf{0}O_j = (A/A_0)^{1/2} \mathbf{R}_j^{(0)},$$

where

$$\mathbf{R}_j^{(0)} = \mathbf{0}O_j^{(0)}. \quad (10)$$

Let us keep each ellipse E_j fixed, its center at O_j and its major axis parallel to Ox . The central ellipse E is allowed to move in the cage of its nearest neighbors. In the orthogonal frame of coordinates xOy , let x and y be the coordinates of the center of el-

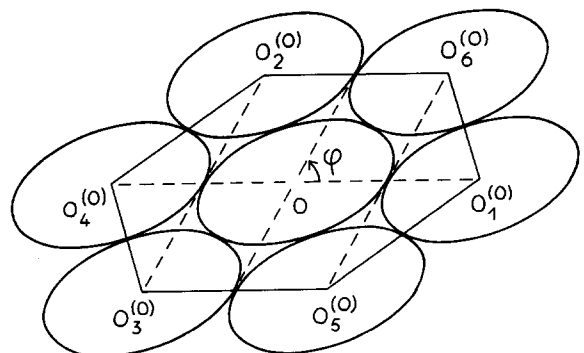


FIG. 2. A close-packed configuration for the hard-ellipse system.

lipse E and θ be the angle of its major axis with Ox [$|\theta| \leq (\pi/2)$]. In configuration space, the partition function associated with ellipse E is

$$Z_1 = \int dx dy d\theta. \tag{11a}$$

The free-volume theory consists of approximating the (configurational) partition function Z_N of the system of ellipses, at density A_0/A , enclosed in a box compatible with the close-packed lattice, by $(Z_1)^N$

$$Z_N \simeq (Z_1)^N. \tag{11b}$$

We show in Appendix F that, as $A \rightarrow A_0$, the displacements x , y , and θ of ellipse E , which appear in the integral (11a), are infinitely small quantities of the same order as the variation of the box size, i.e., as $(A/A_0) - 1$. The partition function Z_1 of ellipse E is therefore an infinitely small quantity of order $[(A/A_0) - 1]^3$. Equation (11b) implies therefore equation (9) with $\nu = 3$. Thus the free-volume theory predicts the value $\nu = 3$ irrespective of the ratio a/b and of the shape of the close-packed lattice.

C. Abnormally Large Displacements at Very High Density

We want to investigate in which way the parameter ν appearing in the asymptotic expressions (8) and (9), that we assume to be valid, depends upon the number of ellipses N , for very large N , for a given value of a/b and a given shape of the box. We always use periodic boundary conditions. To prevent any translation of the system as a whole, we fix the center of ellipse number N at the origin O , which is one of the sites of the close-packed lattice. This constraint does not alter the value of the parameter ν of (9) and (8).

In the close-packed configuration the major axes of all ellipses are parallel to Ox and their centers form a lattice shown on Fig. 2. This lattice is supposed to be unique and to be stable at very high density (Appendix E) taking into account periodic boundary conditions.

One is tempted to assume that, as $A \rightarrow A_0$, the $2N - 2$ coordinates of the displacements of the $N - 1$ moving centers with respect to their lattice sites and the N angles of the major axes of the ellipses with Ox are infinitely small quantities of the same order as the variation of the size of the box, i.e., as $(A/A_0) - 1$, as in the hard-disk case.¹³ If this were true the partition function Z_N of the hard-ellipse system would be an infinitely small quantity equivalent to $[(A/A_0) - 1]^{3N-2}$ and the parameter ν appearing in (9) and (8) would be equal to $3 - (2/N)$.

We however prove in Appendix E, in the case of the close-packed lattice defined by (6a) and (7a), that there exist $2N_x - 1$ independent directions along which the maximum displacements of the ellipses with respect to their lattice sites are infinitely small

quantities of order less than or equal to the order of $[(A/A_0) - 1]^{1/2}$ whereas along all other directions these displacements are of order $[(A/A_0) - 1]$. At very high density these abnormally large displacements along preferred directions increase the partition function Z_N and therefore decrease the pressure. We prove in Appendix E that ν satisfies the following inequalities:

$$3 - (1/N) - (2N_x/N) \leq \nu \leq 3 - (2/N). \tag{12}$$

These inequalities suggest that, whereas translation invariance only lowers the value of ν from the free-volume value $\nu = 3$ by an amount $2/N$ (as in the hard-disk case¹³), these $2N_x - 1$ static collective modes probably lower ν by a quantity $\Delta\nu$ which is of order $1/(N)^{1/2}$ (as is N_x/N) at large values of N for a given value of a/b and a given shape of the box.

As $N \rightarrow +\infty$, the asymptotic expressions (8) and (9) probably remain valid (in a domain of densities A_0/A which does not vanish, for a given accuracy) and the inequalities (12) imply that ν becomes equal to 3.

To prove the existence of the $2N_x - 1$ independent preferred directions introduced above and defined by equalities (E3) and (E4) of Appendix E, no special assumption (of uniqueness and of stability) is necessary: the maximum amplitude of displacements of the ellipses as A approaches A_0 can always be shown to approach zero at least as slowly as $[(A/A_0) - 1]^{1/2}$. In the absence of any assumption of uniqueness and of stability of the lattice there might exist more than $2N_x - 1$ independent preferred directions. In the same way, the second inequality (12) can be proved without these assumptions, for any shape of the box compatible with one of the close-packed lattices of Fig. 2 (taking into account periodic boundary conditions).

All the results of this section and of Appendix E apply of course also in the case where the close-packed lattice is defined by (6b) and (7b), if one permutes the axes Ox and Oy , the numbers N_x and N_y , and a and b .

The existence of these abnormally large displacements at very high density and of a continuous infinity of close-packed configurations for the hard-ellipse system show that ellipses can be more easily "packed" than disks, probably due to their lower symmetry.

IV. THE MONTE CARLO CALCULATION

To study the equilibrium properties of the hard-ellipse system and in particular to determine the equation of state, we use the Monte Carlo method¹ in the canonical ensemble, with periodic boundary conditions. The Statement 2 of Sec. II.A enables us to reject the forbidden configurations of the system, using the contact function of two ellipses $\Psi(\mathbf{r}, \mathbf{u}_1, \mathbf{u}_2; a, b)$ defined by relations (1). The use of the contact function Ψ and of the inequality (3) enables us also to compute the pressure.

A. Calculation of the Pressure

Let \mathbf{r}_j be the position vector of the center of ellipse number j ; \mathbf{u}_j , the unitary vector of its major axis. Let us set $\mathbf{r}_{ij} = \mathbf{r}_j - \mathbf{r}_i$, and let us denote by $\nabla_{ij}\Psi$ the gradient of the contact function $\Psi(\mathbf{r}_{ij}, \mathbf{u}_i, \mathbf{u}_j; a, b)$ with respect to \mathbf{r}_{ij} .

We have shown in Ref. 14, by a straightforward application of the virial theorem,¹⁵ that the compressibility factor PA/NkT is given by the following limit:

$$PA/NkT = \lim_{\Psi_0 \rightarrow 0^+} Z(\Psi_0), \quad (13a)$$

with

$$Z(\Psi_0) = 1 + (1/2N\Psi_0) \langle \sum'_{i<j} |\mathbf{r}_{ij} \cdot \nabla_{ij}\Psi| \rangle; \quad (13b)$$

the average is taken over all allowed configurations; the sum runs over all pairs of ellipses E_i and E_j ($i < j$) such that the contact function $\Psi(\mathbf{r}_{ij}, \mathbf{u}_i, \mathbf{u}_j; a, b)$ be less than the positive number Ψ_0 ; the images of E_i are taken into account.

In the case of hard disks of diameter σ , (13) reduces to the well-known expression deduced from the virial theorem

$$(PA/NkT)_d = 1 + \frac{1}{2}\pi\sigma^2\rho g(\sigma), \quad (14)$$

where $\rho = N/A$ is the density and $g(r)$ is the pair correlation function.

A proof of (13) can be obtained as follows: assume first that the potential through which molecules i and j interact $V_{ij} = V(\mathbf{r}_{ij}, \mathbf{u}_i, \mathbf{u}_j)$ is everywhere continuous, as well as its first derivatives. Call $\rho_{12} = \rho(\mathbf{r}_1, \mathbf{r}_2, \mathbf{u}_1, \mathbf{u}_2)$ the two-body angle dependent distribution function. The virial theorem¹⁵ then yields an expression for the compressibility factor PA/NkT . Let now $V(\mathbf{r}_{12}, \mathbf{u}_1, \mathbf{u}_2)$ tend to infinity when ellipses E_1 and E_2 or their images overlap, and to zero otherwise. Assuming that the quantity $\gamma_{12} = \exp(\beta V_{12})\rho_{12}$ ($\beta = 1/kT$) remains everywhere continuous, unlike both V_{12} and ρ_{12} , and noting that $\mathbf{r}_{12} \cdot \nabla_{12}\Psi$ is positive when the ellipses E_1 and E_2 are exteriorly tangent,¹⁴ one can prove the relation (13).

Since the statistical errors of the Monte Carlo calculation make it difficult to evaluate the limit (13a), we have approximated PA/NkT by the quantity $Z(\Psi_0)$ for some finite but small value of Ψ_0 .

Due to the inequality (3), the only pairs of ellipses that contribute to $Z(\Psi_0)$ are the pairs of ellipses E_i and E_j (taking into account also the images of E_j) such that the distance between their centers be less than some length $r_0 > 2a$ related to the maximum value Ψ_0 of their contact function Ψ_{ij} through the following equation:

$$\Psi_0 = \Psi_d(r_0/a); \quad (15)$$

Ψ_d is the contact function for disks, defined by (2). Thus approximating the limit (13a) by $Z(\Psi_0)$ is analogous to approximating, in the case of hard disks of diameter $\sigma = 2a$, the pair correlation function at

contact $g(\sigma)$ in equation (14) by an integral over a finite shell of width $r_0 - 2a$, i.e., by

$$\frac{2}{r_0^2 - 4a^2} \int_{2a}^{r_0} g(r)rdr.$$

An estimate of the goodness of the approximation made by using a value Ψ_0 to compute the pressure of the hard-ellipse system is therefore the relative width $(r_0/2a) - 1$, where r_0 is related to Ψ_0 through Eq. (15), which would be used in the corresponding approximation in the case of hard disks.

We show in Appendix C that, at density A_0/A , the contact function $\Psi_L(A/A_0)$ associated with two adjacent ellipses of any close-packed lattice is

$$\Psi_L = 3.2^8 (A/A_0)^3 [(A/A_0) - 1]. \quad (16)$$

In order to check the asymptotic expression (8) and to try to determine the parameter ν , we have chosen the value $\Psi_0 = 10^{-2}\Psi_L$ at high density ($A/A_0 < 1.30$). However the statistical errors of the Monte Carlo calculation prevented us from obtaining an accurate enough determination of the limit (13a) and of the parameter ν .

At lower densities ($A/A_0 \geq 1.40$) we have chosen in particular $\Psi_0 = 15.36$, for which $(r_0/2a) - 1 = 10^{-2}$, and a value Ψ_0 4 times bigger, leading to a statistical error on $Z(\Psi_0)$ twice as small; indeed, one can see that, for sufficiently small Ψ_0 and a large enough number of generated configurations, the average value of the sum over pairs of ellipses appearing in the definition of $Z(\Psi_0)$ (13b) is nearly proportional to Ψ_0 [the quantity $Z(\Psi_0)$ varies slightly with Ψ_0] and that the statistical error on this average is therefore proportional to $(\Psi_0)^{1/2}$.

B. Other Technical Aspects of the Calculation

At a given density A_0/A we enclose N ellipses in a rectangular box compatible with one of the close-packed lattices defined by (6a) and (6b). The dimensions of the box are given respectively by (7a) or (7b). We use periodic boundary conditions. Moreover we choose a box as nearly square as possible in order to hinder as little as possible an eventual disorientation of the system.

At each step of the Monte Carlo calculation,¹ we move all the ellipses, one after the other, at random. At each even step we move at random the center of each ellipse in a square of side $2\delta_M$, without changing its orientation. At each odd step we let each ellipse rotate at random around its center in an angular sector $2\theta_M$. We choose δ_M and θ_M in such a way that, on the average, half of the new configurations are accepted and half rejected (such a ratio ensures the fastest convergence).

In the course of the calculation we determine the pressure, in the way indicated above, and the following two quantities:

(a) the structure factor $S(\mathbf{q})$ where \mathbf{q} is one of the basis vectors \mathbf{q}_1 and \mathbf{q}_2 of the reciprocal lattice associated with the lattice of the box (we have taken \mathbf{q}_1 and \mathbf{q}_2 symmetrical with respect to one side of the box):

$$S(\mathbf{q}) = (1/N) \langle \sum_{j,l} \exp[i\mathbf{q} \cdot (\mathbf{r}_j - \mathbf{r}_l)] \rangle. \quad (17)$$

For each configuration, the indices j and l vary independently from 1 to N ; \mathbf{r}_j is the position vector of the center of ellipse number j ; the average is taken over all accepted configurations. In a perfect crystal $S(\mathbf{q})=N$ and, when solid long-range order is destroyed, $S(\mathbf{q})$ becomes of the order of 1.

(b) The directional-order parameter M , defined as

$$M = (1/N^2) \langle \sum_{j,l} \cos(2\theta_j - 2\theta_l) \rangle, \quad (18)$$

where θ_j is the angle between the major axis of ellipse number j and a fixed direction Ox . M is a positive quantity, rotationally invariant, and reaches its maximum value 1 when all the ellipses are perfectly oriented; in a disoriented state, M is of order $1/N$.

We recall that both directional and translational orders probably do not exist strictly at long distance, as in other continuous two-dimensional models.¹⁰ They are order ranging over some hundred ellipses.

All the calculations were made on the UNIVAC 1108 computer at Orsay University.

C. Difficulties in the Case of Hard Ellipsoids

The study of the phase transitions of hard-ellipsoid systems would be of great interest: it is more realistic than a two-dimensional model and leads probably to different phases depending upon the shape, prolate or oblate, of the ellipsoids. Statement 3 of Appendix B gives, in principle, a way of applying the Monte Carlo method to a computation of equilibrium average values of quantity depending only upon the position of the ellipsoids, such as the angle dependent pair correlation function $g(\mathbf{r}, \mathbf{u}_1, \mathbf{u}_2)$, the structure factor, or a directional-order parameter.

However the pressure can no longer be easily evaluated: it is shown in Appendix B (Statement 5) that the relation analogous to (13), with the contact function Ψ of ellipses replaced by the contact function $\Phi(\mathbf{r}, \mathbf{u}_1, \mathbf{u}_2; a, b)$ of ellipsoids, can no longer be helpful. In particular, inequality (3) is of no use in three dimensions, since Φ is everywhere zero in the case of spheres. The length r_0 introduced by (15) is now infinite. More precisely, in the sum (13b), the pair of ellipsoids E_i and E_j can contribute to an infinite number of terms, because of their images: this can be seen, for instance, by choosing an allowed configuration with the axes of E_i and E_j nearly parallel (the contact function Φ_{ij} associated with these images is then nearly zero, due to Statement 5 of Appendix B; in the case of rigid boundary conditions, r_0 is approximately equal to the largest diameter of the box).

One can notice, however, that the function $\mathbf{r} \cdot \nabla \Phi = r(\partial \Phi / \partial r)$, which appears in the sum (13b) instead of $\mathbf{r} \cdot \nabla \Psi$, is zero in all special cases described in Statement 5. It is likely that, as the upper (positive) bound Ψ_0 of Φ approaches zero, the ellipsoids E_i and E_j that contribute most in the sum (13b) are those whose centers (taking into account the images) are closer than some length d which approaches $\max(2a, 2b)$. In order to determine the pressure, one would probably have to study in detail this last behavior.

V. THE TWO-PHASE TRANSITIONS

We have studied the properties of a system of 170 hard ellipses, of axis ratio $a/b=6$, enclosed in a box of nearly square shape compatible with the close-packed lattice defined through (6a) and (7a) with $N_x=5$ and $N_y=34$. As we decrease the density from its maximum value, we first observe the solid oriented phase, then the nematic phase, in which the ellipse axes are still oriented whilst the ellipse centers show no medium-range (nor long-range) order, and last the liquid phase, where there is neither translational nor directional medium-range order. These three phases are separated by two first-order phase transitions.

A. Melting

For an approximately constant number of ellipses N and a nearly fixed shape of the box, the density A_0/A_m at which the solid starts to melt increases when a/b increases. Indeed, at a given density A_0/A , the greater the axis ratio a/b , the more the lattices obtained by expanding the close-packed lattices (shown on Fig. 2) differ from one another. (This difference can be estimated by the structure factor). These lattices can be deduced from one another more easily by making the ellipses slide than by making them rotate as a whole, due to periodic boundary conditions. At a given density A_0/A and for a number N and a shape of box approximately fixed, the close-packed lattice is therefore more and more deformed as a/b increases.

As N tends to infinity the melting density A_0/A_m probably becomes an increasing function of a/b , independent of the shape of the box. In particular, as $a/b \rightarrow +\infty$, the solid and liquid phases vanish and leave place to the nematic phase: $A_m \rightarrow A_0$.

We have observed that at area $A/A_0=1.15$ the system gradually goes from the solid to the nematic phase. After 70 000 steps of the Monte Carlo calculation, the pressure PA_0/NkT , averaged over 10 000 steps (i.e., 1.7×10^6 configurations) increased from 18.8 to 22 while the mean structure factor $\frac{1}{2}[S(\mathbf{q}_1) + S(\mathbf{q}_2)]$, defined by equality (17), dropped regularly from 70 to 10 (Fig. 3). (The positive quantity Ψ_0 was chosen as described in Sec. IV.A; we have checked that with

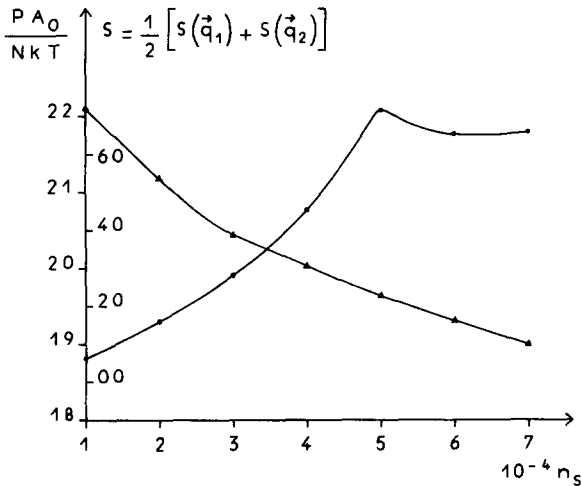


FIG. 3. Transition from the solid phase to the nematic phase at area $A/A_0=1.15$; n_s is the total number of steps of the Monte Carlo calculation.

values of Ψ_0 twice smaller or 4 times bigger we still observe this steep increase of the pressure).

At a smaller area $A/A_0=1.125$ it is very likely that the solid phase is the stable phase: the structure factors $S(\mathbf{q}_1)$ and $S(\mathbf{q}_2)$ averaged over 10 000 steps remain equal to 110 ± 10 after 40 000 steps. We have followed the nematic branch of the isotherm from area $A/A_0=1.15$ and we have gone on to follow the solid branch (Fig. 4). The equation of state of the system at high density is given in Table I; the uncertainty on PA_0/NkT has been estimated from the standard deviation of the pressure averaged over 10 000 steps.

We conclude that the area corresponding to the beginning of the melting A_m/A_0 is certainly smaller than 1.15 (and probably very close to this value) whereas for a system of 870 hard disks⁹ it is as large as 1.266.

B. The Nematic-Liquid Transition

At area $A/A_0=1.40$, we have obtained after 80 000 steps the value 0.7 ± 0.1 for the directional-order parameter M , defined by (18), whereas $S(\mathbf{q})=0.8 \pm 0.4$. The state of the system is therefore one in which the ellipses are still very oriented whilst their centers are completely at random.

The transition from the nematic to the liquid phase is of first order since the "unlocking" of the rotation angles θ_j , which is associated with this transition, leads to a sudden increase of the volume of configuration space available to the system, therefore of the entropy. This geometrical effect is analogous to the "unlocking" of the positions which leads to the melting of the hard-disk system.

However, since the disorientation affects only one degree of freedom per ellipse instead of two in the

melting transition, the nematic and liquid branches of the isotherm are very close to each other. In the transition region the system goes very rapidly from the nematic to the liquid state and inversely, during the course of the calculation; it is very hard to establish a correlation between the variation of the pressure and the variation of the directional-order parameter M .

We have however been able to observe the van der Waals-like loop associated with the disorientation transition (Fig. 5). Using the value $\Psi_0=61.44$ in the calculation of the pressure described in Sec. IV.A, we have managed to obtain several points of this loop. With a step Ψ_0 4 times smaller we have observed very large fluctuations of the pressure in the transition region, so large that they prevented any determination of the isotherm in this region. In the domain of areas $1.40 \leq A/A_0 \leq 2.05$ we have checked that both values of the step Ψ_0 lead to values of PA_0/NkT which are equal within the statistical errors. The use of the larger value $\Psi_0=61.44$ instead of $\Psi_0=15.36$ enabled us to reduce the statistical uncertainty by a factor of 2 and to locate the van der Waals-like loop. On the other hand, we have applied Student's statistical test¹⁶ to averages of the pressure (using $\Psi_0=61.44$) over 10 000 steps (assuming the averages to be statistically independent) and obtained the result that the chance that the pressure decreases when the area A/A_0 increases from 1.775 to 1.7875 is less than 15%.

The disorientation transition (Fig. 5) starts at area $A_d/A_0=1.775 \pm 0.025$. The relative area change at the transition $\Delta A/A$ is probably between 1% and 2%. The corresponding entropy change $\Delta S/Nk$ has a value between 0.05 and 0.12, much smaller than the melting

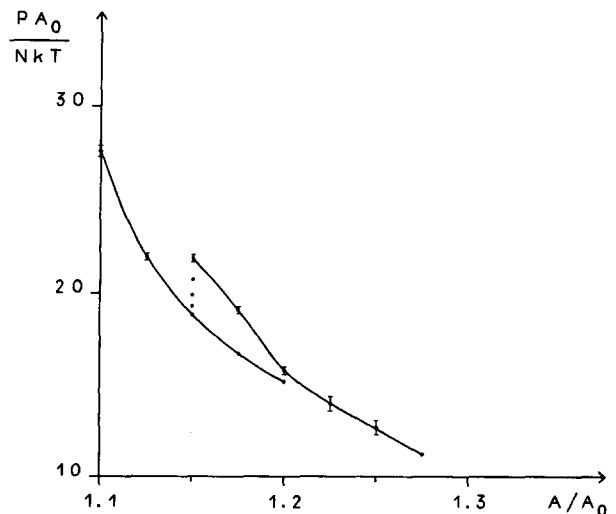


FIG. 4. The solid and nematic branches of the isotherm (for $A/A_0 < 1.30$); we have also shown the transition from the solid to the nematic phase, observed at area $A/A_0=1.15$.

TABLE I. Equation of state at high density.

A/A_0	Solid		Nematic	
	Number of steps	PA_0/NkT	Number of steps	PA_0/NkT
1.10	20 000	27.6 ± 0.3		
1.125	40 000	22.0 ± 0.1		
1.15	10 000	18.8	30 000	21.9 ± 0.2
1.175	10 000	16.7	20 000	19.1 ± 0.2
1.20	30 000	15.2 ± 0.3	20 000	15.8 ± 0.2
1.225			20 000	14.0 ± 0.4
1.25			20 000	12.7 ± 0.4
1.275			10 000	11.2

entropy of hard disks⁹ which is 0.36. Note that $\Delta A/A$ is as small as the relative variation of volume associated with the disorientation transition of a nematic liquid crystal.¹⁷

We have also added to the Hamiltonian of the system an external potential, which can be thought of as an external magnetic field H acting on hypothetical magnetic moments carried by each ellipse

$$V = -H^2 \sum_{j=1}^{j=N} \cos 2\theta_j, \quad (19)$$

where θ_j is the angle of the major axis of ellipse number j with one of the sides of the box, taken as the axis Ox .

For a value $\beta H^2 = 4$, the large fluctuations of the pressure and the disorientation phase transition disappear (Fig. 5) for areas $1.40 \leq A/A_0 \leq 2.0$. The application of a magnetic field H , which orients the ellipses more and more as the density is lower and lower, certainly suppresses the disorientation transition totally (note however that the van der Waals-

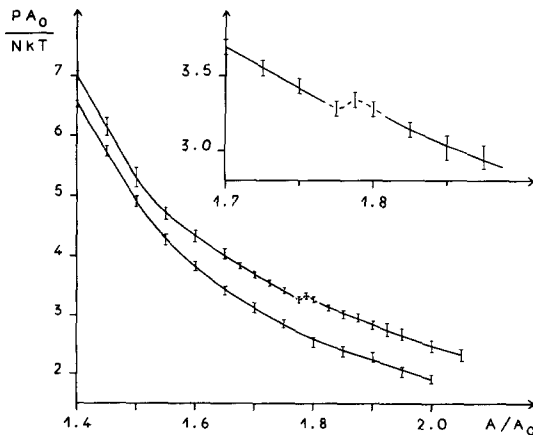


FIG. 5. Isotherms at medium density ($1.4 \leq A/A_0 \leq 2.0$), for zero magnetic field H and for $\beta H^2 = 4$ (lower curve); the nematic-liquid transition region (for $H=0$) is shown at a larger scale.

like loop associated with the transition for zero magnetic field remains for values of the magnetic field $|H|$ which are sufficiently low, and which become lower and lower as the number of ellipses N grows). A very accurate way of determining the free energy of the system, including in the transition region, would be to stabilize the nematic phase by applying a magnetic field. This would however require longer calculations.

It is likely that, as the magnetic field $|H|$ increases, for any axis ratio a/b , number of ellipses N and shape of the close-packed lattice, the melting area A_m/A_0 increases. In particular, as $|H| \rightarrow +\infty$, all the major axes become parallel to Ox and the system behaves

TABLE II. Equation of state at medium density.

A/A_0	$H=0$		$\beta H^2=4$	
	Number of steps	PA_0/NkT	Number of steps	PA_0/NkT
1.40	80 000	7.00 ± 0.07	20 000	6.52 ± 0.05
1.45	20 000	6.15 ± 0.15	10 000	5.74 ± 0.07
1.50	20 000	5.31 ± 0.15	10 000	4.91 ± 0.07
1.55	20 000	4.70 ± 0.10	10 000	4.26 ± 0.07
1.60	30 000	4.33 ± 0.10	10 000	3.82 ± 0.07
1.65	70 000	4.04 ± 0.07	10 000	3.42 ± 0.07
1.675	40 000	3.84 ± 0.05		
1.70	50 000	3.69 ± 0.05	10 000	3.14 ± 0.07
1.725	40 000	3.55 ± 0.05		
1.75	80 000	3.43 ± 0.05	10 000	2.85 ± 0.07
1.775	80 000	3.28 ± 0.05		
1.7875	80 000	3.34 ± 0.05		
1.80	80 000	3.28 ± 0.05	10 000	2.54 ± 0.07
1.825	80 000	3.14 ± 0.05		
1.85	40 000	3.02 ± 0.08	10 000	2.39 ± 0.07
1.875	40 000	2.96 ± 0.08		
1.90	40 000	2.84 ± 0.08	10 000	2.29 ± 0.07
1.925	20 000	2.76 ± 0.10		
1.95	20 000	2.67 ± 0.10	10 000	2.04 ± 0.07
2.00	30 000	2.48 ± 0.10	20 000	1.93 ± 0.05
2.05	20 000	2.32 ± 0.10		

exactly as a hard-disk system, as can be seen by applying the affinity (4).

The equation of state of the ellipse system at medium densities ($1.40 \leq A/A_0 \leq 2.0$) is given in Table II. The value of Ψ_0 chosen to determine the pressure (Sec. IV.A) was 61.44 for $H=0$ and 15.36 for $\beta H^2=4$ (in the latter case, we checked that using a value of Ψ_0 4 times bigger leads to a value of PA_0/NkT which differs by less than 0.1). The statistical uncertainty on PA_0/NkT has been estimated by the standard deviation of the average of the pressure over 10 000 steps for $H=0$ and over 5000 steps for $\beta H^2=4$.

The directional-order parameter M , defined by (18), is shown on Fig. 6 for $H=0$ and for $\beta H^2=4$. In zero

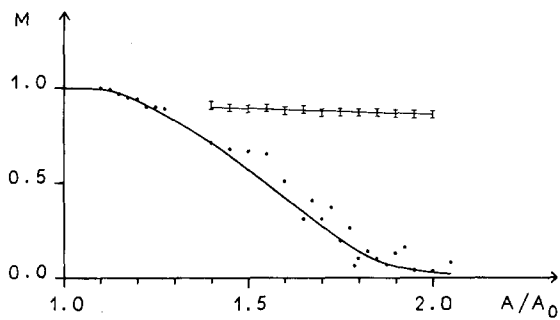


FIG. 6. Variation of the directional-order parameter M with A/A_0 for zero magnetic field H (black circles) and for $\beta H^2=4$ (dots with error bars).

magnetic field, we were unable to determine accurately M since its statistical fluctuations are of much larger relative amplitude than the fluctuations of the pressure and range over a number of steps at least 8 times greater.

This difference in the behavior of M and of the pressure can be understood as follows: in a given configuration, all ellipses contribute to M , whereas only pairs of neighboring ellipses, which are very often nearly independent of each other, contribute to the pressure.

It seems that even after the nematic-liquid transition there remains a very weak residual orientation of the ellipses, due to the small size of the system.

C. Phases of the System for Weak and Very Strong Elongations

If the axis ratio a/b is sufficiently close to 1, when the density decreases, the system undergoes a disorientation transition before melting. We expect to observe a phase analogous to the plastic crystal phase^{11,12} with ellipses completely disoriented but whose centers form a lattice.

In order to observe such a phase, we have studied a system of 168 hard ellipses, with axis ratio $a/b=1.01$, at area $A/A_0=1.15$ [the box, almost square, was compatible with the lattice defined by (6b) and (7b), with $N_x=14$ and $N_y=12$]. After 30 000 steps, i.e., 5×10^6 configurations, the structure factors $S(\mathbf{q}_1)$ and $S(\mathbf{q}_2)$, averaged over 10 000 steps, remained equal to 140 ± 10 whereas the directional-order parameter has the value: $M=0.006 \pm 0.001$. The system is therefore completely disoriented but still solid.

On the contrary, as a/b grows to infinity, the melting transition probably occurs at a density infinitely close to the close-packed density and the disorientation transition starts at an area A_d/A_0 which is infinite: the only remaining phase is the nematic phase. We prove in Appendix D that, for N infinitely long ellipses, the nematic-liquid transition area A_d/A_0 tends to infinity as $(1/2\sqrt{3})(a/b)(A_{hr}/N)$ where A_{hr} is the

corresponding area of the disorientation transition which is likely to occur in a system of N hard rods of length 2 (enclosed in a box of the same shape as the box used for the ellipses, with periodic boundary conditions) as is suggested by Onsager's theory.⁶ (A_d can be determined by Maxwell's double-tangent construction; note that this hard-rod transition is not necessarily of first order.)

VI. CONCLUSION

We have shown that in a system of 170 hard ellipses of axis ratio $a/b=6$, two first-order phase transitions occur:

(a) a solid-nematic transition, starting at a density A_0/A_m significantly higher than the density at which the hard-disk system starts to melt;

(b) a nematic-liquid transition, starting at area $A_d/A_0=1.775 \pm 0.025$ and occurring with an entropy change $\Delta S/Nk$ 3 to 7 times smaller than the melting entropy of the hard-disk system.

This result suggests that the nematic-liquid transition of real liquid crystals, as the melting transition, might be mainly due to geometrical factors.

Besides, we have studied the asymptotic behavior of the hard-ellipse pressure and free energy at very high density. We have shown that, as the area of the system approaches its smallest value, there are some preferred directions along which the maximum allowed displacements of the ellipses are much larger than along others. Because of these static collective modes, the asymptotic behavior probably differs from the one predicted by the free-volume theory by a (negative) quantity of order $1/(N)^{1/2}$, for large values of the number N of ellipses, instead of $-2/N$ as for hard disks.

Let us finally state some of the interesting questions which remain and which would need further investigation: A more accurate determination of the entropy change at the nematic-liquid transition could be obtained by studying the free energy in presence of a magnetic field. A detailed analysis of the directional-order parameter M should be made, especially for large values of N . The two-dimensional system of hard rods of finite length might deserve an investigation, since it probably shows a disorientation transition. Finally a study of the three-dimensional hard-ellipsoid system would probably be most interesting: it will probably be shown, if we overcome the technical difficulties that we have described, a difference between the phase transitions of a system of oblate ellipsoids and those of a system of prolate ellipsoids.

ACKNOWLEDGMENTS

I am grateful to Dr. D. Levesque for his considerable help in the numerical work, to Professor P.-G. de Gennes, Professor B. Jancovici, Professor L. Verlet,

and Professor J. Yvon and to Dr. J.-P. Hansen and Dr. D. Schiff for helpful discussion. I wish to thank Mr. Johannin and the operation staff of the UNIVAC 1108 computer in Orsay University, Mrs. S. Bonnevey, Dr. W. Theumann, and Dr. J. Ginibre for their kind cooperation.

APPENDIX A: OUTLINE OF THE PROOF OF STATEMENTS 1 AND 2

We consider the ellipses E_1 and E_2 defined in Sec. II.A. Their equations are ($\alpha=1, 2$)

$$F_\alpha(M) \equiv [(0_\alpha M \cdot u_\alpha)^2/a^2] + [(0_\alpha M \cdot u_{\alpha'})^2/b^2] - 1 = 0. \tag{A1}$$

Let M_i ($i=1, \dots, 4$) be their intersection points (real or complex, distinct or not). Let us consider the pencil of conics¹⁸ generated by E_1 and E_2 , i.e., the family of conics $C(\lambda)$ with equation

$$F(\lambda, M) \equiv F_1(M) + \lambda F_2(M) = 0, \tag{A2}$$

where λ is a complex parameter.

This pencil contains three degenerate conics C_1, C_2 , and C_3 , which consist of the pairs of straight lines (M_1M_2, M_3M_4) , (M_1M_3, M_2M_4) , and (M_1M_4, M_2M_3) , respectively. The corresponding values of λ , namely $\lambda_1, \lambda_2, \lambda_3$, are the roots of the determinant of $C(\lambda)$ which equals

$$P(\lambda) = \lambda^3 + f_1\lambda^2 + f_2\lambda + 1 \tag{A3}$$

up to a constant factor. The coefficients f_1 and f_2 are those given by Eq. (1b).

Using geometrical arguments one can prove¹⁴ the following correspondence between the configurations of the pair of ellipses E_1 and E_2 and the properties of the roots λ_1, λ_2 , and λ_3 of $P(\lambda)$:

Case 1: Ellipses E_1 and E_2 are tangent (at a real point); $P(\lambda)$ possesses a multiple root.

Case 2: E_1 and E_2 have no real common point; the roots of $P(\lambda)$ are real and distinct, and they are not all negative.

Case 3: E_1 and E_2 intersect at four distinct real points; the roots of $P(\lambda)$ are real, distinct and negative.

Case 4: E_1 and E_2 have only two distinct real common points; $P(\lambda)$ possesses two complex conjugate roots.

To complete the proof of Statements 1 and 2 we express the discriminant of $P(\lambda)$, i.e., the product $P(\mu_1)P(\mu_2)$ where μ_1 and μ_2 are the roots of $P'(\lambda)$, in terms of f_1 and f_2 . The contact function Ψ of E_1 and E_2 is precisely the quantity $[-81P(\mu_1)P(\mu_2)]$. From this definition of Ψ and Eq. (A3), we deduce very easily the following statements: $P(\lambda)$ possesses a multiple root if and only if $\Psi=0$. The necessary and sufficient condition for the roots of $P(\lambda)$ to be real and distinct is $\Psi>0$. If the roots of $P(\lambda)$ are

real, they are all negative if and only if f_1 and f_2 are positive.

Applying these remarks to the four cases described above, we easily obtain Statements 1 and 2 (and similar statements for Cases 3 and 4).

APPENDIX B: THE CONTACT FUNCTION OF TWO IDENTICAL ELLIPSOIDS OF REVOLUTION

Let us consider two identical ellipsoids of revolution E_1 and E_2 . Let O_1 and O_2 be their centers; u_1 and u_2 , the unitary vectors of their axes of revolution. The length of each ellipsoid along its axis of revolution is $2a$ and their larger transverse size equals $2b$. We set $r = [[O_1O_2]]$.

Using methods similar to those of Appendix A, we have shown in Ref. 14 the following statement, analogous to Statement 2 of Sec. II.A, which enables us to reject the forbidden configurations of the hard-ellipsoid system in the Monte Carlo calculation.

Statement 3. The necessary and sufficient condition for two ellipsoids E_1 and E_2 to have no real point in common or to be exteriorly tangent is that the three following functions Φ, S_1 , and S_2 be positive or zero and that one at least among the quantities g_1, g_2 , and h be negative.

g_α ($\alpha=1$ or 2) and h are the following functions of r, u_1, u_2, a and b —(u_1, u_2, r) is the scalar triple product $(u_1 \times u_2) \cdot r$ —

$$g_\alpha = 4 + [(a/b) - (b/a)]^2 (u_1 \times u_2)^2 - (r^2/b^2) + [(1/b^2) - (1/a^2)] (r \cdot u_\alpha)^2, \tag{B1a}$$

$$h = g_1 + g_2 - 2 - (1/b^2) [(a/b) - (b/a)]^2 (u_1, u_2, r)^2. \tag{B1b}$$

If we set

$$p = -h, \tag{B2a}$$

$$q = g_1 g_2 - 4, \tag{B2b}$$

$$w = 4h - g_1^2 - g_2^2, \tag{B2c}$$

Φ, S_1 , and S_2 are the following functions of r, u_1, u_2, a and b

$$\Phi = 4(p^2 - 3q)(q^2 - 3wp) - (9w - pq)^2, \tag{B3a}$$

$$S_1 = h^2 - 2g_1 g_2 - 4, \tag{B3b}$$

$$S_2 = g_1^2 g_2^2 + 8g_1 g_2 - 2h(g_1^2 + g_2^2). \tag{B3c}$$

The following statement shows that $\Phi(r, u_1, u_2; a, b)$ plays indeed the role of the contact function for ellipsoids.

Statement 4. When two ellipsoids E_1 and E_2 are tangent (interiorly or exteriorly), their contact function Φ is zero.

But, contrary to the contact function of ellipses, that of ellipsoids Φ , can be zero though the ellipsoids

are not tangent at any real point (however they are then tangent at two imaginary conjugate points). Indeed, we have proved in Ref. 14 the following statement.

Statement 5. When two ellipsoids E_1 and E_2 have no real common point, the necessary and sufficient condition for their contact function Φ to be zero is that their axes of revolution and the line of centers O_1O_2 be coplanar and that the quantities $|\mathbf{r}\cdot\mathbf{u}_1|$ and $|\mathbf{r}\cdot\mathbf{u}_2|$ be equal.

Moreover this condition is sufficient, even when the ellipsoids overlap, as we can verify directly by using equations (B1), (B2), and (B3a). In particular Φ is zero when the axes of revolution of the ellipsoids are parallel. The contact function is identically zero in the case of spheres ($a=b$).

APPENDIX C: VALUES OF Ψ WHEN THE MAJOR AXES OF THE ELLIPSES ARE PARALLEL

Let us use the notations of Sec. II.A. When the major axes of ellipses E_1 and E_2 are parallel $\mathbf{u}_1=\mathbf{u}_2=\mathbf{u}_0$ and $\mathbf{u}'_1=\mathbf{u}'_2=\mathbf{u}'_0$. In this case, let x and y be the coordinates of the vector $\mathbf{r}=\llbracket 0,0_2 \rrbracket$ in the orthogonal frame $(\mathbf{u}_0, \mathbf{u}'_0)$. Let us set

$$s = (x^2/a^2) + (y^2/b^2). \tag{C1a}$$

From equalities (1), the functions $f_1, f_2,$ and Ψ can be written as follows

$$f_1(\mathbf{r}, \mathbf{u}_0, \mathbf{u}_0) = f_2(\mathbf{r}, \mathbf{u}_0, \mathbf{u}_0) = 3 - s = f \tag{C1b}$$

$$\Psi(\mathbf{r}, \mathbf{u}_0, \mathbf{u}_0) = 3(f-3)^3(f+1) = 3s^3(s-4). \tag{C1c}$$

In particular, when E_1 and E_2 are two adjacent ellipses of the lattice shown on Fig. 2, the contact function Ψ is zero; the quantities s and f take the following values

$$s = s^{(0)} = 4, \tag{C2a}$$

$$f = f^{(0)} = -1. \tag{C2b}$$

Let us apply the similarity of center 0 and ratio $(A/A_0)^{1/2}$ to the sites of this lattice (Fig. 2), keeping the axes of the ellipses constant in magnitude and direction. In the case of two nearest neighbor ellipses, the function s equals $4A/A_0$, according to (C1a) and (C2a). At area A/A_0 , the contact function Ψ relative to two adjacent ellipses therefore takes the following value Ψ_L

$$\Psi_L(A/A_0) = 3.2^8(A/A_0)^3 [(A/A_0) - 1]. \tag{C3}$$

APPENDIX D: THE NEMATIC-LIQUID TRANSITION WHEN a/b APPROACHES INFINITY

In this appendix we shall prove the following result, quoted in Sec. V.C; when a/b approaches infinity, the area A_d/A_0 at which the nematic-liquid transition

starts (or ends) is an infinitely large quantity equivalent to the expression $(1/2\sqrt{3})(a/b)(A_{hr}/N)$, where the area A_{hr} corresponds to the disorientation transition which probably occurs in a system of N hard rods of length 2, enclosed in a box of the same shape, with also periodic boundary conditions.

Let us then consider a system of N hard ellipses. Let \mathbf{r}_j be the position vector of the center of ellipse E_j (with respect to the origin 0). Let us increase a to infinity keeping b fixed. Let us set

$$\mathbf{r}_j = a\boldsymbol{\rho}_j, \tag{D1a}$$

$$\boldsymbol{\rho} = \boldsymbol{\rho}_2 - \boldsymbol{\rho}_1. \tag{D1b}$$

In this limit let us investigate whether the ellipses E_1 and E_2 , for instance, do not overlap, by using Statement 2 of Sec. II.A and Equalities (1). When $a \rightarrow +\infty$, the functions f_α ($\alpha=1$ or 2) are almost everywhere infinitely large quantities equivalent to $(a^2/b^2)[\sin^2\theta - (\boldsymbol{\rho}\cdot\mathbf{u}'_\alpha)^2]$ and the contact function Ψ is an infinitely large quantity equivalent to $3f_1^2f_2^2$.

Therefore, in this limit, the necessary and sufficient condition for ellipses E_1 and E_2 to overlap is that both quantities $\sin^2\theta - (\boldsymbol{\rho}\cdot\mathbf{u}'_\alpha)^2$ be positive or zero. It is just the overlap condition of two hard rods of length 2, respectively parallel to \mathbf{u}_1 and \mathbf{u}_2 , and whose center position vectors are $\boldsymbol{\rho}_1$ and $\boldsymbol{\rho}_2$. Thus we associate N hard rods with the ellipses.

From Equality (D1a), if the disorientation transition, which is likely to occur in the N hard-rod system, starts at area A_{hr} , that of ellipses starts at area A_d , which is an infinitely large quantity equivalent to a^2A_{hr} . Using Equality (5) (where $\rho_0=N/A_0$), we find therefore the behavior of the relative area A_d/A_0 when a/b approaches infinity.

APPENDIX E: PREFERRED DIRECTIONS OF DISPLACEMENTS AT VERY HIGH DENSITY

I. Description of the Preferred Directions

In this Appendix, we shall essentially show the existence of the abnormally large allowed displacements of the ellipses at very high density, which we have introduced in Sec. III.C. To this end, we shall use ideas of Salsburg and Wood¹³ about hard disks at very high density.

Let us first consider any shape of the lattice shown on Fig. 2. At area A/A_0 , we define the position 0_j of the N lattice sites by Eqs. (10), but now the index j runs from 1 to N . Let \mathbf{r}_j be the position vector of the center of ellipse number j E_j (with respect to the origin 0) and θ_j the angle (modulo π) of its major axis with Ox ; if \mathbf{u}_j is the unitary vector of this major axis and \mathbf{u}_0 is that of the axis Ox ,

$$\boldsymbol{\theta}_j = (Ox, \mathbf{u}_j) = (\mathbf{u}_0, \mathbf{u}_j), \tag{E1a}$$

with $|\theta_j| \leq \pi/2$. We set also

$$\Delta \mathbf{r}_j = \mathbf{r}_j - \mathbf{R}_j. \tag{E1b}$$

The center of ellipse E_N is still at the origin 0; $\mathbf{r}_N = \mathbf{R}_N = \mathbf{0}$.

In each configuration of the system, we number the $N-1$ other ellipses in order to minimize the sum

$$\sum_{k=1}^{k=N-1} (\Delta \mathbf{r}_k)^2.$$

Let Δx_j and Δy_j be the components of the vector $\Delta \mathbf{r}_j$, in the orthogonal frame of coordinates Oxy . Let us make the following coordinate transformation

$$\Delta x_j = \sigma a \xi_j, \tag{E2a}$$

$$\Delta y_j = \sigma b \eta_j, \tag{E2b}$$

$$\theta_j = \sigma [(a/b) - (b/a)]^{-1} \tau_j, \tag{E2c}$$

with

$$\sigma = \left[\sum_{k=1}^{k=N} \frac{\Delta x_k^2}{a^2} + \frac{\Delta y_k^2}{b^2} + \left(\frac{a}{b} - \frac{b}{a} \right)^2 \theta_k^2 \right]^{1/2}. \tag{E2d}$$

Let ζ_j be the vector whose components are ξ_j and η_j in the frame of coordinates $Oxy(\zeta_N=0)$. The point $D = (\zeta_1, \dots, \zeta_{N-1}, \tau_1, \dots, \tau_{N-1}, \tau_N)$ belongs to the unit sphere of the $(3N-2)$ -dimensional space. D and σ stand, respectively, for the direction and the amplitude of the displacements of the ellipses, from their respective positions on the lattice.

Let us now consider the lattice defined by conditions (6a) and (7a). We assume that this lattice is unique and above all stable: As the area A approaches A_0 , σ tends uniformly to zero. It can however happen that the box containing the ellipses is compatible with several lattices, defined for instance by (6a) and (6b). If these lattices are completely disconnected at very high density, we can consider each of them separately.

Using these assumptions we shall show the existence of preferred directions D , along which the maximum amplitude $\sigma_M(D, A/A_0)$ of the (allowed) displacements of the ellipses, at area A/A_0 , is an infinitely small quantity of order less than or equal to the order of $[(A/A_0)-1]^{1/2}$, when A tends to A_0 , whereas σ_M is of order $(A/A_0)-1$ in every other direction D . (Omitting the assumptions of stability and of uniqueness of the lattice, we shall obtain slightly weaker results.)

Let $X_j^{(0)}$ and $Y_j^{(0)}$ be the coordinates (in the frame Oxy) of the site $0_j^{(0)}$ of the lattice at maximum density ($X_N^{(0)} = Y_N^{(0)} = 0$) and let \mathbf{u}_0' be the unit vector of the axis Oy . These preferred directions D are generated by the $2N_x-1$ independent directions defined as follows, by means of the phases $\Phi_j^{(\mu)}$ ($\mu=1, 2, \dots, 2N_x-1$)

$$\Phi_j^{(\mu)} = (m\pi/N_x)(1/a)X_j^{(0)} + \phi_\mu, \tag{E3a}$$

$$\zeta_j^{(\mu)} = \frac{1}{2}A_\mu \cotg(m\pi/2N_x) [\sin\Phi_j^{(\mu)} - \sin\phi_\mu] \mathbf{u}_0', \tag{E3b}$$

$$\tau_j^{(\mu)} = A_\mu \cos\Phi_j^{(\mu)}; \tag{E3c}$$

the integer m runs from 1 to N_x ; $\phi_\mu=0$ or $\pi/2$ for $1 \leq m < N_x$; $\phi_\mu=0$ if $m=N_x$; the real coefficient A_μ is a normalization constant.

Each preferred direction is defined by the following linear equations (where $\delta_1=2N_x-1$)

$$\zeta_j = \sum_{\mu=1}^{\mu=\delta_1} B_\mu \zeta_j^{(\mu)}, \tag{E4a}$$

$$\tau_j = \sum_{\mu=1}^{\mu=\delta_1} B_\mu \tau_j^{(\mu)}; \tag{E4b}$$

the $2N_x-1$ real constants B_μ verify the normalization condition

$$\sum_{j=1}^{j=N-1} (\zeta_j^2 + \tau_j^2) + \tau_N^2 = 1.$$

In these preferred directions all the displacements of the ellipse centers are perpendicular to the initial direction of their major axes Ox .

In the case of the lattice defined by (6a) and (7a), after showing the existence of these abnormally large displacements, we shall be able to prove the first inequality (12). This inequality is due to the existence of the $2N_x-1$ static collective modes (E3), which increase the (configurational) partition function Z_N at very high density and reduce the pressure and the constant ν . As we shall now see, the proof of the second inequality (12) is much simpler and much more general than the proof of the first one: It applies to any shape of the lattice shown on Fig. 2, without any assumption of stability or of uniqueness.

II. Proof of the Second Inequality (12)

In the limit as the area A tends to A_0 , we shall therefore investigate, by means of Statement 2 and Eqs. (1), whether the configuration (σ, D) of the N ellipses is allowed. For the moment we consider any shape of the lattice (Fig. 2). We first assume that this lattice is unique and stable at very high density.

At maximum density, Eqs. (4) transform the site $0_j^{(0)}$ of the hard-ellipse lattice (Fig. 2) into the site $0_j'^{(0)}$ of the lattice formed by the N hard disks of unit radius (Fig. 1). We recall that $\mathbf{R}_j^{(0)} = \llbracket 00_j^{(0)} \rrbracket$, let us set

$$\mathbf{R}_{jk}^{(0)} = \mathbf{R}_k^{(0)} - \mathbf{R}_j^{(0)} \tag{E5a}$$

$$\mathbf{R}_{jk}'^{(0)} = \mathbf{R}_k'^{(0)} - \mathbf{R}_j'^{(0)} \text{ with } \mathbf{R}_j'^{(0)} = \llbracket 00_j'^{(0)} \rrbracket. \tag{E5b}$$

According to (4), in the frame Oxy , the coordinates $X_{jk}^{(0)}$ and $Y_{jk}^{(0)}$ of $\mathbf{R}_{jk}^{(0)}$ are related to the components $X_{jk}'^{(0)}$ and $Y_{jk}'^{(0)}$ of $\mathbf{R}_{jk}'^{(0)}$ in the following way

$$X_{jk}^{(0)} = aX_{jk}'^{(0)}, \quad Y_{jk}^{(0)} = bY_{jk}'^{(0)}. \tag{E6}$$

Let us set

$$c_{jk} = \frac{1}{2}X_{jk}'^{(0)}Y_{jk}'^{(0)}. \tag{E7}$$

Using Statement 2, we determine now if the ellipses E_j and E_k do not overlap (taking into account periodic

boundary conditions). When $A \rightarrow A_0$, σ tends uniformly to zero; $f_\alpha(\mathbf{r}_k - \mathbf{r}_j, \mathbf{u}_j, \mathbf{u}_k)$ (for $\alpha=1$ or 2) tends uniformly to $f_\alpha(\mathbf{R}_{jk}^{(0)}, \mathbf{u}_0, \mathbf{u}_0)$ which is less than or equal to -1 as can be seen from Eqs. (C1) and (C2). Besides, the contact function $\Psi_{jk} \equiv \Psi(\mathbf{r}_k - \mathbf{r}_j, \mathbf{u}_j, \mathbf{u}_k)$ tends uniformly to $\Psi_{jk}^{(0)} \equiv \Psi(\mathbf{R}_{jk}^{(0)}, \mathbf{u}_0, \mathbf{u}_0)$ which is always positive or zero. $\Psi_{jk}^{(0)}$ is zero if and only if the sites $0_j^{(0)}$ and $0_k^{(0)}$ (or their images) are nearest neighbors. Therefore, in the limit as $A \rightarrow A_0$, it follows from Statement 2 that the allowed configurations of ellipses (σ, D) are given by " $\Psi_{jk} > 0$ for any pair of adjacent sites $0_j^{(0)}$ and $0_k^{(0)}$ ".

For fixed area A , when the amplitude of displacements σ tends to zero, the functions $\Psi_{jk}(\sigma, D, A/A_0)$ associated with pairs of adjacent sites tend uniformly to the quantity $\Psi_L(A/A_0)$ defined by Eq. (C3). Let us therefore write

$$(3^{-1})(2^{-7})\Psi_{jk} = 2(A/A_0)^3[(A/A_0) - 1] - \sigma l_{jk}(\sigma, D, A/A_0); \quad (E8)$$

the function l_{jk} is everywhere continuous and indefinitely differentiable, even for $\sigma=0$. When $A \rightarrow A_0$, σ tends uniformly to zero and $l_{jk}(\sigma, D, A/A_0)$ tends uniformly to

$$L_{jk}(D) = (-3^{-1})(2^{-7})[(\partial/\partial\sigma)\Psi_{jk}]_{0,D,1}. \quad (E9)$$

To determine $L_{jk}(D)$, we use Ψ_{jk} and Eqs. (E1), (E2), (10), (1), (C2b), (E6), and (E7). We obtain in that way

$$L_{jk}(D) = (\zeta_j - \zeta_k) \cdot \mathbf{R}_{jk}^{(0)} + c_{jk}(\tau_j + \tau_k). \quad (E10)$$

Let $l(\sigma, D, A/A_0)$ be the greatest of the $3N$ numbers l_{jk} associated with pairs of adjacent sites

$$l(\sigma, D, A/A_0) = \max_{j < k} [l_{jk}(\sigma, D, A/A_0)]. \quad (E11)$$

Therefore, according to (E8), in the limit as $A \rightarrow A_0$, the necessary and sufficient condition for the configuration (σ, D) to be allowed is

$$2(A/A_0)^3[(A/A_0) - 1] - \sigma l(\sigma, D, A/A_0) > 0. \quad (E12)$$

Let us now prove the second inequality (12). From Eqs. (E2) we deduce that the configurational partition function Z_N of the system of ellipses can be written as follows (if translations of E_N are allowed)

$$Z_N = (A/ab)[a^2b^2/(a^2 - b^2)]^N \int \sigma^{3N-3} d\sigma d\Omega(D), \quad (E13)$$

in this integral $d\Omega(D)$ is the element of area on the unit sphere of the $(3N-2)$ -dimensional space.

Let M be a positive upper bound of $l(\sigma, D, A/A_0)$ for σ and A/A_0 less than two, for any direction D . According to (E12), for any $\sigma < (2/M)[(A/A_0) - 1]$, the configuration (σ, D) is allowed. We note that the latter statement can be proved without any assumption of stability or of uniqueness of the hard-ellipse lattice, since the values σ considered in this statement necessarily tend to zero uniformly when

$A \rightarrow A_0$. Thence, from Eq. (E13) it follows that Z_N is greater than $K_1[(A/A_0) - 1]^{3N-2}$, where K_1 is a constant. From Eq. (9) we deduce the second inequality (12).

III. Proof of the Existence of the Preferred Directions

Let $\sigma_M(D, A/A_0)$ be the lower upper bound of the allowed values of the amplitude σ , along any given direction D of displacements. To define σ_M , particularly in the case where the box containing the ellipses is compatible with several lattices, we can only consider the configurations (σ, D) "accessible"¹³ from the configuration $\sigma=0$, which are obtained as follows: We suppose that the ellipses first occupy their respective positions on the lattice defined by the condition $\sigma=0$. Then we make all the continuous deformations of the system so that no two ellipses overlap (D is not fixed). We thus generate the configurations (σ, D) accessible from the configuration $\sigma=0$.

We shall now study the behavior of σ_M when $A \rightarrow A_0$. Inequality (E12) involves the following equation

$$2(A/A_0)^3[(A/A_0) - 1] - \sigma_M l(\sigma_M, D, A/A_0) = 0. \quad (E14)$$

Let $L(D)$ be the greatest of the $3N$ quantities $L_{jk}(D)$ defined by Eq. (E9) and associated with pairs of adjacent sites

$$L(D) = \max_{j < k} [L_{jk}(D)]. \quad (E15)$$

Let us now use the assumption of stability of the hard-ellipse lattice. From Eqs. (E11), (E8), (E9), and (E15) we deduce that, when A tends to A_0 , $l(\sigma_M, D, A/A_0)$ tends uniformly to $L(D)$. Consequently, from Eq. (E14), it follows that the ratio $\sigma_M/[(A/A_0) - 1]$ tends to $2/L(D)$. If $L(D)$ is positive, σ_M is therefore an infinitely small quantity of order $(A/A_0) - 1$, as is the variation of the size of the box containing the ellipses. When $L(D)$ is zero, σ_M is an infinitely small quantity of order less than the order of $(A/A_0) - 1$; the allowed displacements in direction D are then abnormally large at very high density. In the latter case, by continuing the expansion (E8) of Ψ_{jk} in powers of σ , we could show that the order of σ_M is less than or equal to the order of $[(A/A_0) - 1]^{1/2}$.

We shall now verify that $L(D)$ is everywhere positive or zero. The hexagonal symmetry of the hard-disk lattice (Fig. 1) and Eqs. (E5b) and (E7) yield the following equalities, where the sums run over the six sites $0_k^{(0)}$ adjacent to any given site $0_j^{(0)}$

$$\sum_k \mathbf{R}_{jk}^{(0)} = \mathbf{0} \quad \text{and} \quad \sum_k c_{jk} = 0. \quad (E16a)$$

Therefore, from Eq. (E10) we deduce that the $3N$ linear forms $L_{jk}(D)$ associated with pairs of adjacent

sites satisfy the following identity

$$\sum'_{j < k} L_{jk}(D) = 0. \tag{E16b}$$

According to the latter equality and Eq. (E15), $L(D)$ is positive or zero. $L(D)=0$ if and only if the $3N$ linear forms $L_{jk}(D)$ are zero. The preferred directions of displacements at very high density are therefore given by the set of the $3N$ homogeneous linear equations $L_{jk}(D)=0$, with $\zeta_N=0$ since the center of ellipse E_N is at the origin 0.

We shall now solve this set of linear equations. Let us consider the quantities $\mathbf{R}_{jk}'^{(0)}$ and c_{jk} appearing in Eq. (E10). According to Eqs. (E5b) and (E7), $\mathbf{R}_{jk}'^{(0)}$ and c_{jk} are invariant under translation of both sites $0_j'^{(0)}$ and $0_k'^{(0)}$ on the hard-disk lattice (Fig. 1). For this reason we make the following Fourier transformation (with $1 \leq j \leq N$)

$$\zeta_j = \sum_{\mathbf{q}} \exp(i\mathbf{q} \cdot \mathbf{R}_j'^{(0)}) \zeta(\mathbf{q}), \tag{E17a}$$

$$\tau_j = \sum_{\mathbf{q}} \exp(i\mathbf{q} \cdot \mathbf{R}_j'^{(0)}) \tau(\mathbf{q}); \tag{E17b}$$

the N vectors \mathbf{q} belong to the reciprocal lattice of the box containing the N hard disks of unit radius (we assume that the sides of this box are respectively parallel to $00_1'^{(0)}$ and to $0_3'^{(0)}0_2'^{(0)}$ on Fig. 1). As $\zeta_N = \mathbf{R}_N'^{(0)} = 0$, the sum of the Fourier components $\zeta(\mathbf{q})$ is zero.

In the particular case of the hard-ellipse lattice defined by (6a) and (7a), straightforward but rather long calculations thus yield¹⁴ the preferred directions of displacements (E3) and (E4).

We note that the existence of these static collective modes (corresponding to particular values of \mathbf{q}) can be proven without any assumption of stability or of uniqueness of the hard-ellipse lattice. Indeed, along any preferred direction D , the ratio $\sigma_M / [(A/A_0) - 1]$ tends to infinity even if σ_M does not tend to zero. In the absence of these assumptions there might exist other preferred directions of displacements and the first inequality (12) might be false.

IV. Proof of the First Inequality (12)

Let us now prove this inequality, still in the particular case of the lattice defined by (6a) and (7a). Let I be the origin ($\sigma=0$) of the $(3N-2)$ -dimensional configuration space V . In this space, with each configuration (σ, D) we associate the vector $[[IP]] = \sigma[[ID]]$. Replacing $[[ID]]$ by $[[IP]]$ in Eqs. (E10) and (E15) we can still define the linear forms $L_{jk}(P) = L_{jk}([[IP]])$ and the function $L(P)$.

Let us consider points P_1 satisfying the condition $L(P_1)=0$, i.e., the $3N$ equations $L_{jk}(P_1)=0$. Vectors $[[IP_1]]$ generate a linear vector subspace V_1 of V . From Eqs. (E4), the dimension of V_1 is $\delta_1=2N_x-1$. Let V_2 be the linear vector subspace orthogonal to V_1 ;

the dimension of V_2 is $\delta_2=3N-2N_x-1$. Let us project $[[IP]]$ on subspaces V_1 and V_2 ; $[[IP]] = [[IP_1]] + [[IP_2]]$ (the vector $[[IP_2]]$ belongs to V_2). We shall now prove that the magnitude IP_2 is an infinitely small quantity of order greater than or equal to the order of $(A/A_0)-1$, when $A \rightarrow A_0$, along a given direction D .

Let μ_2 be the unit vector parallel to $[[IP_2]]$. The definitions of subspaces V_1 and V_2 and Eq. (E15) yield the identity $\sigma L(D) = L(P) = IP_2 L(\mu_2)$, where $L(\mu_2)$ is everywhere positive. In the limit as $A \rightarrow A_0$, according to Eq. (E14), the quantity $\sigma L(D) = L(P)$ is (approximately) less than $2[(A/A_0)-1]$. Since $L(P) = IP_2 L(\mu_2)$, when $A \rightarrow A_0$, IP_2 and the δ_2 coordinates of P_2 in V_2 (with respect to any basis of vectors spanning V_2) tend to zero at least as fast as $(A/A_0)-1$. Since IP_1 is bounded, the partition function Z_N is less than $K_2[(A/A_0)-1]^{\delta_2}$, where K_2 is a constant. As $\delta_2=3N-2N_x-1$, from Eq. (9) we deduce the first inequality (12).

APPENDIX F: PROOF OF THE RESULT $\nu=3$ IN THE FREE-VOLUME APPROXIMATION

In this appendix we indicate how the result quoted at the end of Sec. III.B can be proved¹⁴ by using methods of Appendix E. We now consider, at area A , the ellipse E and its six fixed nearest neighbors E_j (with $1 \leq j \leq 6$) defined in Sec. III.B. We investigate whether ellipse E and any of the ellipses E_j do not overlap and we proceed along the lines of Appendix E with the following slight modifications.

The system now includes seven ellipses, six of the ellipses are fixed. Ellipse E_N (with $N=7$) coincides with E (the center of E_N is no longer at the origin). The coordinates appearing in Eqs. (E2) are

$$\Delta x_j = \Delta y_j = \theta_j = 0, \quad \text{for } 1 \leq j \leq 6,$$

$$\Delta x_N = x, \quad \Delta y_N = y, \quad \text{and } \theta_N = \theta.$$

The point D belongs to the unit sphere of the three-dimensional configuration space. The assumptions of stability and of uniqueness quoted at the beginning of Appendix E are now unnecessary.

The analogue of the quantity $L(D)$ defined by Eq. (E15) is now the greatest of six linear forms $L_j(D)$ associated with the six fixed ellipses E_j (for $1 \leq j \leq 6$). We can deduce $L_j(D)$ from Eq. (E10) by letting the site $0_k'^{(0)}$ coincide with the origin. According to Eq. (E16b), the sum of the six functions $L_j(D)$ is identically zero. But, since these quantities cannot be altogether zero on the unit sphere, $L(D)$ is now everywhere positive. Therefore, when $A \rightarrow A_0$, the maximum amplitude $\sigma_M(D, A/A_0)$ of displacements (of ellipse E) along the direction D is an infinitely small quantity equivalent to $2[(A/A_0)-1]/L(D)$. The coordinates x , y , and θ are infinitely small quantities of order $(A/A_0)-1$.

* Postal address, Laboratoire de Physique Théorique et Hautes Energies, Bat. 211, Faculté des Sciences, 91 ORSAY, France.

† Laboratoire associé au C.N.R.S.

¹ W. W. Wood and F. R. Parker, *J. Chem. Phys.* **27**, 720 (1957).

² A. Rahman, *Phys. Rev.* **136**, A405 (1964).

³ L. Verlet, *Phys. Rev.* **159**, 98 (1967); **165**, 201 (1968).

⁴ B. J. Alder and T. E. Wainwright, *J. Chem. Phys.* **33**, 1439 (1960).

⁵ I. G. Chistyakov, *Usp. Fiz. Nauk* **89**, 563 (1966) [*Sov. Phys. Usp.* **9**, 551 (1967)].

⁶ L. Onsager, *Phys. Rev.* **62**, 558 (1942); *Ann. N.Y. Acad. Sci.* **51**, 627 (1949).

⁷ A. Ishihara, *J. Chem. Phys.* **19**, 1142 (1951).

⁸ R. Zwanzig, *J. Chem. Phys.* **39**, 1714 (1963).

⁹ B. J. Alder and T. E. Wainwright, *Phys. Rev.* **127**, 359 (1962).

¹⁰ L. D. Landau and E. M. Lifshitz, *Statistical Physics*, (Pergamon, New York, 1959), pp. 409-412.

¹¹ D. Fox, M. M. Labes and A. Weissberger, *Physics and Chemistry of Organic Solid State* (Interscience, New York, 1963-1965), Vol. 1, p. 89.

¹² *J. Phys. Chem. Solids* **18**, 1 (1961) (Proceedings of a symposium held in Oxford University in April 1960).

¹³ Z. W. Salsburg and W. W. Wood, *J. Chem. Phys.* **37**, 798 (1962).

¹⁴ J. Vieillard-Baron, thèse de Doctorat d'Etat, Faculté des Sciences d'Orsay, 1970.

¹⁵ K. Huang, *Statistical Mechanics* (Wiley, New York, 1965), p. 150.

¹⁶ D. B. Owen, *Handbook of Statistical Tables* (Addison-Wesley, Reading, Mass., 1962), p. 41.

¹⁷ E. Bauer and J. Bernamont, *J. Phys. Radium* **7**, 19 (1936).

¹⁸ G. Cagnac, E. Ramis and J. Commeau, *Nouveau Cours de Mathématiques Spéciales* (Masson, Paris, 1965), Vol. 3, p. 481.

THE JOURNAL OF CHEMICAL PHYSICS

VOLUME 56, NUMBER 10

15 MAY 1972

INDO and MINDO/2 Crystal Orbital Study of Polyacetylene, Polyethylene, and Polyglycine

DAVID L. BEVERIDGE AND ISSAM JANO

Department of Chemistry, Hunter College of the City University of New York, New York, New York 10021

AND

JANOS LADIK

Central Research Institute for Chemistry of the Hungarian Academy of Sciences, Budapest, Hungary

(Received 7 December 1971)

Approximate valence electron self-consistent field crystal orbital calculations using INDO and MINDO/2 parameters are described for polyacetylene, polyethylene, and polyglycine in a planar and α -helical conformation. The electronic energy band structure and electronic charge distribution are discussed and compared with previous theoretical calculations and available experimental results.

I. INTRODUCTION

It has been recognized for some years now that a useful perspective on the electronic structure of organic and biological macromolecules may be derived from the energy band theory of solid state physics. The quasiperiodic core potential of the macromolecular backbone gives rise to a manifold of energy levels resembling that expected for a one-dimensional crystal, with bands of levels separated by forbidden zones or bandgaps. The bandgap ΔE between the highest filled and lowest unfilled bands and the band shapes define theoretical values for the intrinsic electrical conductivity of the system.

The theoretical description of polymers as with other large organic molecules was first approached in the framework of the π -electron approximation, using free electron theory¹ and independent electron molecular orbital theory² to simplify the computations to a tractable level. The Huckel theory of organic quantum chemistry has been applied extensively to polymeric systems, notably by Lennard-Jones,³ Longuet-Higgins and Salem,⁴ Tsuji, Huzinaga and Hasino,⁵ and Kutzelnigg.⁶ Studies using advanced methods were reported by Ooshika⁷ and Dewar and Gleicher,⁸ and

Pople and Walmsley.⁹ Studies on polypeptides were reported by Evans and Gergeley,¹⁰ Yomosa,¹¹ Suard, Berther and Pullman,¹² and Suard-Sender.¹³

The series of papers by Ladik and co-workers¹⁴ have detailed the application of independent electron and self-consistent field crystal orbital theory in the π -electron approximation, with extensive applications to the calculation of π -bands in periodic models of nucleic acids. A parallel series of papers by Andre, Gouverneur, and Leroy¹⁵ have treated the electronic structure of polyene, polyacenes, and graphite from a similar viewpoint.

The interplay between the theoretical studies on the electronic structure of polymers and the experimental work on properties such as electrical conductivity has to date been very constructive and significant. The bandgap for a two-dimensional polypeptide network was calculated by Suard-Sender to be ~ 5 eV against an experimentally measured value of ~ 2.4 eV and appeared to rule out intrinsic semiconductivity as the conduction method. Reconsideration of the relationship between calculated and observed values recognizing the experiments were carried out in a medium with a dry state dielectric constant ~ 3 indicated that the Suard-Sender value was not neces-